

## Performance Analysis Using CFD Code of the Reactor Coolant Pump for the APR1400

Ja Y. GU<sup>a</sup> and Kune Y. SUH<sup>a,b\*</sup>

<sup>a</sup>PHILOSOPHIA, Inc., 599 Gwanak-Ro, Gwanak-Gu, Seoul, 151-744, Korea

<sup>b</sup>Seoul National University, 599 Gwanak-Ro, Gwanak-Gu, Seoul, 151-744, Korea

\*Corresponding author: kysuh@snu.ac.kr

### 1. Introduction

The Reactor Coolant Pump (RCP) circulates the coolant from the reactor to the steam generators and back to the reactor under high temperature and high pressure conditions. The coolant transmits massive thermal energy produced in the core to the secondary system in the SGs. The RCP design thus requires much more sophisticated analysis than the ordinary pump design.

Difficulties surfaced in domesticating the relevant technology, while the Doosan Heavy Industries & Construction Co. (DHIC) endeavors to develop the RCP technology for the APR1400. The engineering calls for an industrial scale investment to develop a pump to operate at high pressure and high temperature. In this study the analysis using a computational fluid dynamics (CFD) is discussed of the RCP performance in the nominal operating condition.

### 2. CFD analysis

#### 2.1. Pump modeling and meshing

The RCP shown in Fig. 1 has 6 impeller blades and 11 diffuser blades and it is mixed-flow pump designed by DHIC. ANSYS BladeGen<sup>TM</sup> is utilized to generate analysis models for the impeller and diffuser.

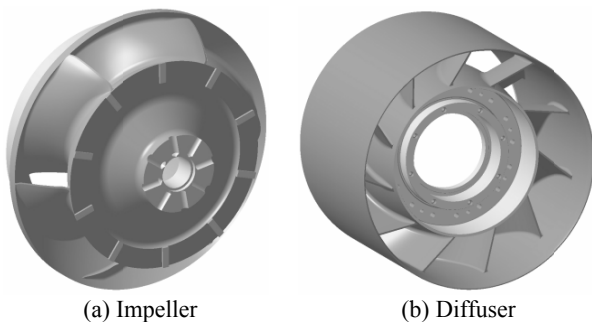


Fig. 1 RCP 3D modeling for APR1400

The grids of the pump are meshed as structured grid system by ANSYS TurboGrid<sup>TM</sup>. A total of 543,300 grids are used for numerical analysis of the pump. Fig. 2 indicates meshed blades.

#### 2.2. CFD analysis

The computational analysis is executed by ANSYS CFX<sup>®</sup> by employing the Reynolds averaged Navier-Stokes equations as governing equations to examine incompressible turbulent flow. The high resolution

scheme is used as derivation technique, while the Shear Stress Transport (SST)  $k-\omega$  based model is used to account for turbulence.

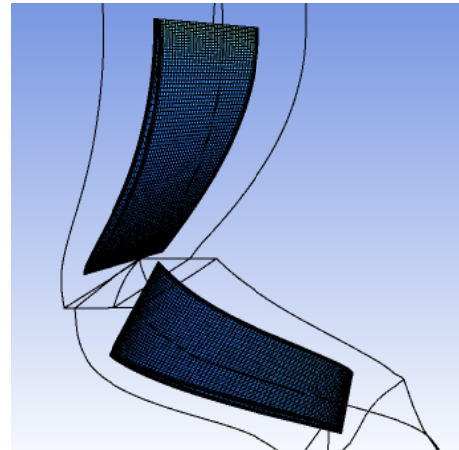


Fig. 2 Coupled blades of the impeller and diffuser assembly

The boundary condition is based on the nominal operating condition of APR1400 as listed in Table 1. The inlet and outlet of the pump are distanced from the actual points because accurate flow states cannot be observed in a short flow field.

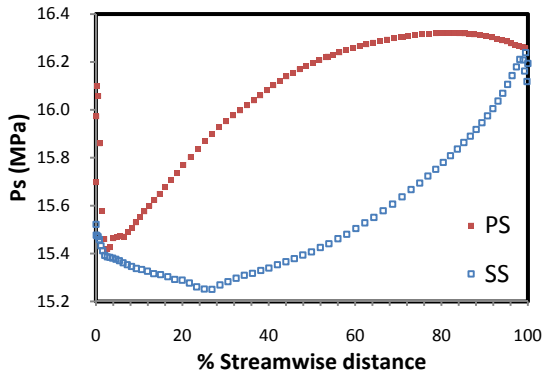
Table 1. RCP Boundary Conditions

Parameter	Design	Operation
Inlet total pressure [MPa]	17.6	15.6
Temperature [°C]	343	290.6
Outlet mass flow rate [m <sup>3</sup> /s]	5719.44	
Working fluid	Water	

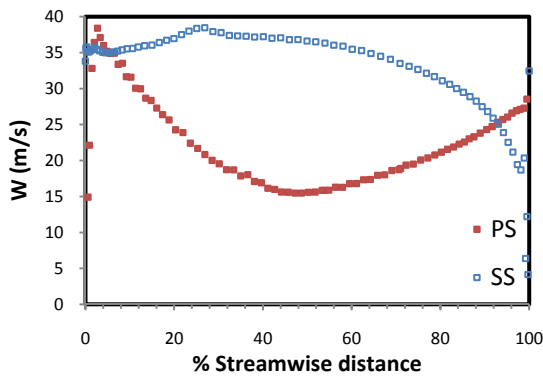
### 3. Results and discussion

Figs. 3(a) and 3(b) show each static pressure blade loading and relative velocity distribution at span 50% of the impeller blade. In Fig. 3(a) the static pressure blade loading is distributed smoothly. In Fig. 3(b) for the relative velocity distributions, two lines regarding velocity distributions on pressure surface (PS) and on suction surface (SS) cross at a point of streamwise about 92%. The relative velocity distributions take on the form  $\hookleftarrow$  according to Breambussche[1]. The crossing of two lines as shown in Fig. 3(b) thereupon obstructs smooth flow of the fluid and causes the pump efficiency to decrease. There are a couple of reasons for this phenomenon. One is inappropriate distribution of the impeller blade angle and thickness. The other has to do with the impeller's outlet angle. Since a large outlet angle brings separation and stall of flow at rear of the

impeller, the distorted flow decreases the momentum of fluid as it is mixed with the nominal flow as shown in Fig. 3



(a) Static pressure blade loading at the impeller



(b) Relative velocity distribution at the impeller

Fig.3 Detailed performance characteristics of the RCP at the operating condition

In the performance curves dimensionless variables are applied to more effectively express different combinations of several physical values such as volume flow rate ( $Q$ [m<sup>3</sup>/s]), rotational velocity ( $\omega$ [rad/s]), total head ( $H$ [m]), density ( $\rho$ [kg/m<sup>3</sup>]) and shaft power ( $P_{\text{shaft}}$ [W]).  $\phi$ ,  $\psi$ ,  $\tau$  and  $\eta$  mean respectively the flow coefficient, pressure coefficient, power coefficient and pump efficiency and are calculated [2,3] as.

$$\phi = \frac{10 \times Q}{\omega D_{2t}^3} \quad (1)$$

$$\psi = \frac{10 \times gH}{\omega^2 D_{2t}^2} \quad (2)$$

$$\tau = \frac{100 \times P_{\text{shaft}}}{\rho \omega^3 D_{2t}^5} \quad (3)$$

$$\eta = \frac{\rho gQH}{P_{\text{shaft}}} \quad (4)$$

Fig. 4 presents these values given the flow coefficient. The maximum efficiency is 84.64% at flow coefficient 0.496. The efficiency at the operating point is 84.16%. The total head is 9.5 m larger than the net positive

suction head (NPSH) of the RCP, and the creation of cavitations will be prevented.

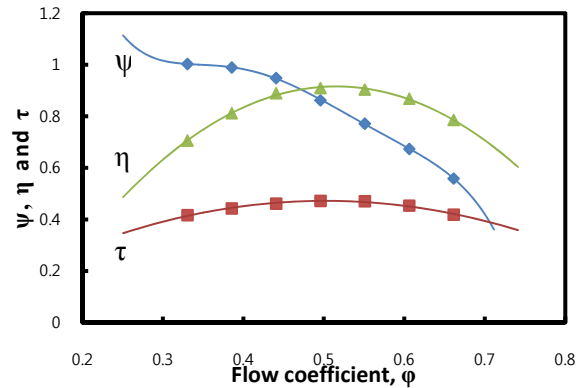


Fig. 4 Performance characteristic curve

#### 4. Conclusions

The pump performance is analyzed at the off-design points. It is an extension from previous analysis at the operating and design points.

The result of this analysis is regarded as appropriate from the standpoint of performance curves of a general mixed-flow pump for the most part. Low flow region has difficulties concerning convergence for numerical analysis.

Results from this study may be used for experimental setup of the RCP. The results will help operate the RCP in APR1400 as well.

#### REFERENCES

- [1]R.A. Breambussche, (Ed.) "Application of inverse methods to 3D turbine and compressor blade design," Turbomachinery Blade Design Systems, VKI Lecture Series 1999-02, Von Karman Institute for Fluid Dynamics, Brussels, Belgium, 1999.
- [2]H.W. Oh, E.S. Yoon, J.S. Ha, M.K. Chung, "Performance prediction of mixed-flow pumps," *J. Mechanical Science and Technology*, Part B Vol. 22, No. 1, pp. 70-78, 1998.
- [3]H.W. Oh, E.S. Yoon, J.W. Ahn, "Design and performance analysis of mixed-flow pumps for waterjet marine propulsion," *J. Fluid Machinery*, Vol. 6, No. 2, pp. 41-46, 2003.